Proc. Natl. Acad. Sci. USA
Vol. 94, pp. 724–728, January 1997
Neurobiology

Dendritic calcium conductances generate high-frequency oscillation in thalamocortical neurons

(thalamus/dendrites/*in vitro*/gamma band frequency/calcium currents)

CHRISTINE PEDROARENA AND RODOLFO LLINÁS

Department of Physiology and Neurosciences, New York University Medical Center, New York, NY 10016

Contributed by Rodolfo Llinás, November 18, 1996

ABSTRACT **Cortical-projecting thalamic neurons, in guinea pig brain slices, display high-frequency membrane potential oscillations (20–80 Hz), when their somata are depolarized beyond −45 mV. These oscillations, preferentially located at dendritic sites, are supported by the activation of P/Q type calcium channels, as opposed to the expected persistent sodium conductance responsible for such rhythmic behavior in other central neurons. Short hyperpolarizing pulses reset the phase and transiently increase the amplitude of these oscillations. This intrinsic thalamic electroresponsiveness may serve as a cellular-based temporal binding mechanism that sharpens the temporal coincidence of cortical-feedback synaptic inputs, known to distribute at remote dendritic sites on thalamic neurons.**

The intrinsic electrophysiological properties of thalamic neurons are among the richest in the central nervous system (1–3). In addition to the membrane mechanisms responsible for spike generation and synaptic transmission present in most nerve cells, thalamic neurons express several types of voltage-gated sodium, potassium, and calcium conductances that are responsible for the complex excitability patterns that these cells demonstrate (2, 4). High-frequency spontaneous membrane oscillations (near 40 Hz) have been described in projection (5, 6) and reticular thalamic neurons (7). Such near 40 Hz oscillations were originally shown at sparsely spinous interneurons of the frontal cortex where the oscillations are dependent on the activation of a persistent sodium conductance (8). Here we report that in thalamocortical neurons (TCNs), calcium conductances, located preferentially at remote dendritic sites, rather than sodium conductances, are responsible for such high-frequency membrane potential oscillations. A short communication on these results has been presented (9).

MATERIALS AND METHODS

The electrophysiological and Ca^{2+} imaging results reported here were performed in adult guinea pig thalamic slices. Slicing and recording techniques were the same as those used in previous research in this laboratory (1). Briefly, adult guinea pigs (150–250 g) were anesthetized with Nembutal (30 mg/kg) and decapitated. Using a vibratome, coronal slices (350–400 μm), were prepared from a block of tissue containing the thalamus and associated cortex such that thalamocortical connectivity was maintained. The slices were cut under cold (6–10°C) oxygenated Ringer's solution, allowed to recover for 1–2 hr, and then transferred to a recording chamber superfused with a solution containing 126 mM NaCl, 5 mM KCl, 26 mM $NaHCO_3$, 13 mM $MgSO_4$, 12 mM KH_2PO_4, and 10 mM glucose saturated with 95% O_2/5% CO_2. Recordings were performed at 35°C. In experiments where the ionic medium was modified, control solutions contained 130 mM NaCl, 6.2 mM KCl, 1.3 mM $MgCl_2$, 10 mM glucose, 25 mM Hepes and saturated with 100% O_2. In the sodium free solutions, NaCl was substituted on equimolar bases by choline chloride. When Cd^{2+}, Mg^{2+}, CO^{2+}, and Ba^{2+} were added in concentrations exceeding 0.2 mM, Ca^{2+} was omitted or reduced in equimolar amounts to maintain constant the total divalent concentration. The ion blockers tetrodotoxin (TTX) (Sigma, 1 mg/ml) and tetraethylammonium·Cl (Sigma, 0.5–5 mM) were added to the normal superfusing medium. When the concentration exceeded 1 mM, the concentration of NaCl was equimolarly reduced from the solution. The stock solutions of the calcium channels blockers were: synthetic analog of the funnel web spider toxin (sFTX), peptidyl toxin from *Agelenopsis aperta* (kindly provided by N. A. Sacomano, Pfizer Pharmaceuticals), and toxin from *Conus geographus* (Alomone Labs) were prepared in distilled water and the drugs were then applied directly to the bath. Nicardipine·HCl (Sigma) was diluted in 100% ethanol and then added to the superfusing medium. The final concentration of ethanol never exceeded 0.01% in the perfusing medium. Direct illumination was avoided during the management of nicardipine.

Intracellular recordings were obtained from TCNs located in several dorsal thalamic nuclei including the intralaminar nucleus. Sharp glass microelectrodes filled with 3 M potassium acetate and 40–80 MΩ of resistance were used in all recordings. Signals were amplified (Axoclamp 2A), digitized (Neurocorder), and stored on a videotape recorder for off-line analysis. Relay TCNs were identified by their antidromic invasion from cortical stimulation sites.

To study the changes in the spatial distribution of intracellular Ca^{2+} concentration, thalamic cells were filled, after somatic penetrations, with the fluorescent pentapotassium Fura-2 (10 mM). Fluorescence images obtained with excitation at 380 nm were stored using a high-speed video system (10). Imaging of the relative calcium concentration was obtained by subtracting control images from those obtained during high-frequency oscillatory activity (10).

RESULTS

Intracellular recordings presented correspond to 75 TCNs selected on the bases of their resting membrane potential (≤ -60 mV), located in different dorsal thalamic nuclei. In all cases studied, oscillatory activity could be triggered by membrane depolarization to levels beyond −45 mV (±4 mV). Most of the neurons ($n = 52$) demonstrated oscillation frequencies ranging from 25 to 50 Hz, but frequencies from 15 to 65 Hz were observed in the whole sample of neurons. Typically, thalamic neurons fire repetitively (Fig. 1*A Right*) when depo-

The publication costs of this article were defrayed in part by page charge payment. This article must therefore be hereby marked "*advertisement*" in accordance with 18 U.S.C. §1734 solely to indicate this fact.

0027-8424/97/94724-5$2.00/0
PNAS is available online at **http://www.pnas.org**.

Abbreviations: sFTX, synthetic analog of the funnel web spider toxin; TTX, tetrodotoxin; TCN, thalamocortical neurons.

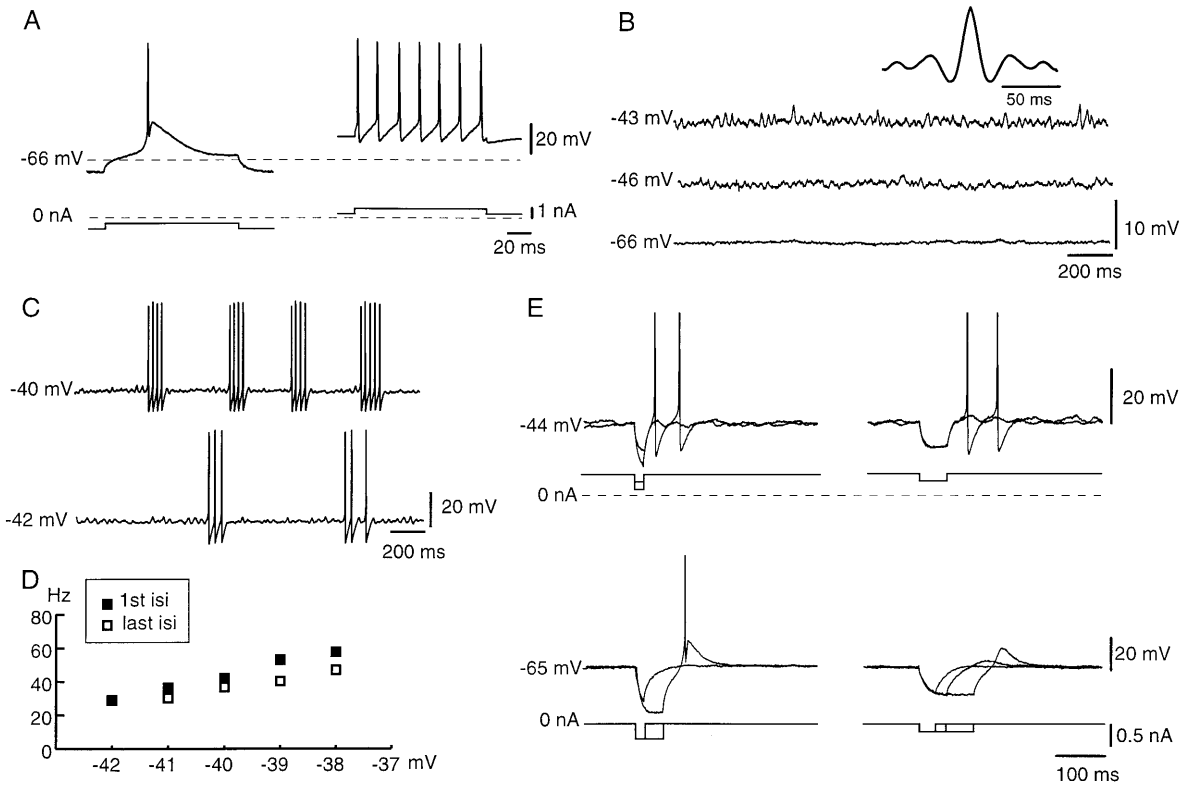

FIG. 1. Fast oscillations in TCNs. (*A*) Direct activation of a thalamic cell from two levels of membrane potential. The labeled −66-mV broken line indicates the resting membrane potential. (*B*) In the same cell, subthreshold oscillations at two different levels of membrane potential induced by outward dc injection. The dominant frequency at −43 mV was 37.5 Hz (see *Inset*, autocorrelogram). (*C*) High-frequency trains of spikes induced by increasing dc injection. Note that the spikes are triggered at the same frequency as the subthreshold oscillations. (Filtering of the traces at 2 kHz reduced the amplitude of the spikes.) (*D*) Corresponding graph of discharge frequency vs. membrane potential. The rate of discharges are in the gamma band. isi, inter-spike interval. (*E*) Oscillations are reset (upper traces) by brief hyperpolarizations induced by the injection of short-duration inward current pulses. (Lower traces) Low-threshold spikes can be induced by outward current pulses of longer duration or higher amplitudes than those in upper traces, even from resting membrane potential (−65 mV).

larized beyond −37 mV (1). If the membrane potential was made negative to −65 mV, direct activation generates a low-threshold calcium spike (Fig. 1*A Left*) that triggered the typical thalamic spike bursts (1, 2). Depolarization to levels positive to −46 mV was accompanied by subthreshold membrane potential oscillations (Fig. 1*B*). The amplitude of this rhythmic activity waxed and waned with time (Fig. 1*B*). Further depolarization was accompanied by single spike activity riding on the oscillatory potentials (Fig. 1*C*), and exhibiting firing rates in the gamma band (Fig. 1*D*).

Oscillatory Reset by Transient Membrane Hyperpolarization. A very significant property of the fast subthreshold oscillatory activity consists of being resetable by short hyperpolarizing current pulses. Current injections mimicking the amplitude and time course of the rapid $GABA_A$ inhibitory postsynaptic potentials generated by local interneurons or by reticular thalamic neurons (7, 11) are followed by a reset of the oscillatory activity. Examples of this rebound are shown in the upper traces of Fig. 1*E*. Note that the phase of the subthreshold oscillation is reset by the hyperpolarizations and that spikes are triggered on the rising phase of the oscillation. The frequency of the oscillation preceding the reset was in all cases comparable to that following the reset. This reset occurs at membrane potential levels (≥−61 mV) too shallow and short lasting to deinactivate the low-threshold calcium conductances in these neurons (1). As shown in Fig. 1*E* (lower traces), longer and larger hyperpolarizations are required to induce a low-threshold spike, even from resting membrane potential.

Ionic Mechanisms Underlying the Subthreshold Oscillation. *Sodium conductances.* A set of experiments was implemented to determine the ionic bases for such oscillation. Since high-frequency oscillation has been associated with persistent sodium conductances [gNa(p)] (8, 12), TTX, known to block gNa(p) (13), was added to the bath and the oscillatory properties of the cells were tested (Fig. 2*A Left*). TTX did not block the oscillatory properties of thalamic neurons (Fig. 2*A Right*) in 12 neurons tested. Thus, the persistent sodium current responsible for high-frequency oscillations in other cells (8, 12) is not responsible for this intrinsic thalamic oscillation.

Since it has been reported that sodium conductances in central neurons may be TTX-insensitive (14), experiments were implemented in which sodium was replaced by choline chloride in the superfusion fluid. In these experiments, as in the case of the TTX, no obvious change in the oscillatory ability of neurons was seen in three of four neurons examined (Fig. 2*C*). These results clearly demonstrate that the high-frequency oscillation does not require the activation of a voltage-gated sodium ionic conductance. It was evident from the results however that the gNa(p) facilitated dendritic depolarizations of somatic origin. Indeed, the threshold for the membrane oscillation increased to 2–7 mV in the presence of TTX or when sodium was replaced by choline in the superfusion fluid (Fig. 2*A* Left). This was demonstrated directly by measuring the effective resistance of the neuron using step depolarizing pulses (Fig. 2*B*). Thus, the decrease in amplitude and time constant of the resulting voltage step indicated a significant reduction in the effective input resistance in the absence of gNa(p).

Calcium conductances. A second set of experiments was designed to test the role of calcium in membrane potential oscillation. Cadmium (0.2 mM) was added to the superfusate to block voltage-gated calcium channels. As shown in Fig. 2*D*

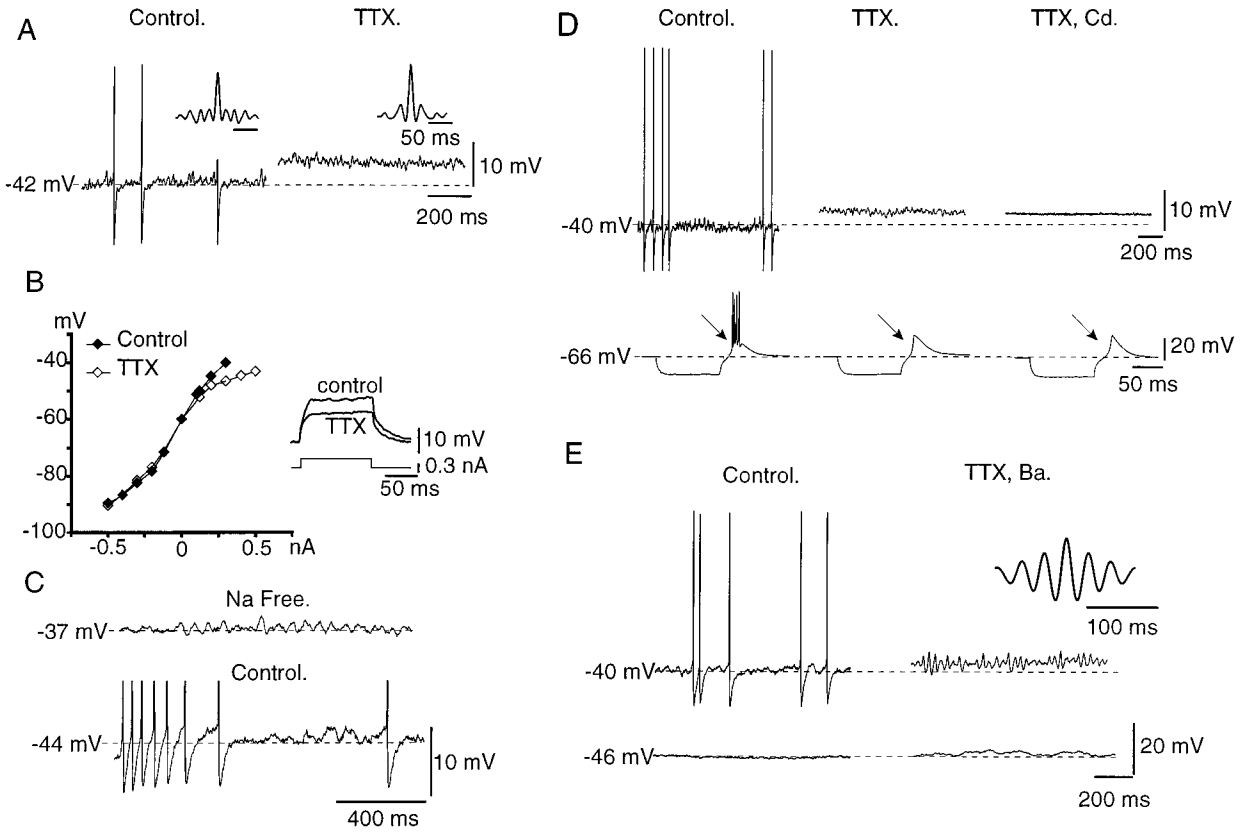

FIG. 2. Ionic mechanisms of the fast subthreshold membrane potential oscillation in thalamocortical cells. (*A*) TTX did not block oscillation, but increased voltage threshold (*Insets*, autocorrelograms). (*B*) Plot of voltage responses to outward and inward current pulses from −60 mV, before and after TTX. Following TTX, the effective depolarization decreased (*Inset*) and a strong outward rectification for membrane potentials positive to −50 mV became evident. (*C*) NaCl equimolar substitution with choline chloride did not block oscillation. (*D*) $CdCl_2$ (up to 0.2 mM) blocked the fast subthreshold membrane potential oscillations but not the low-threshold spikes (arrows). (*E*) Fast subthreshold oscillations became more evident after equimolar replacement of $CaCl_2$ by $BaCl_2$.

(*Right*, upper trace) cadmium blocked high-frequency oscillation. It, however, had no effect on the low-threshold calcium dependent spikes (Fig. 2*D Right*, lower trace) characteristic of these neurons (2). This finding indicates that the oscillatory properties were not due to the activation of a remote T-type calcium channel. Removal of calcium from the extracellular milieu and substitution by cobalt resulted in a complete disappearance of the oscillatory activity. Replacement of calcium by barium in the extracellular milieu was followed by an increase in the amplitude of the oscillatory events, which reached a steady state within 15 min (Fig. 2 *D Right*), demonstrating that barium can serve as a charge carrier for thalamic oscillations (15). However, a decrease in the peak frequency of the oscillatory event for given membrane potential was observed in barium, suggesting that this ion probably had some blocking effect on potassium conductances. Barium also produced a decrease in the threshold voltage for oscillation (Fig. 2*E Right*), most probably due to the increased dendritic length constant occurring as a further consequence of the barium dependent potassium conductance block. These later results suggested that the calcium conductance responsible for thalamic oscillation could be located at some distance from the current injection site, probably at the dendrites.

Identification of Calcium Channel Type. Pharmacological criteria were used to determine the type of calcium channel responsible for such oscillation (Fig. 3). Application of the N-type calcium channel blocker ω-CgTx (16) in concentrations of 1–10 μM or the L-type channel blocker dihydropyridines (16) (nicardipine) at up to 2 μM fail to block such oscillations (Fig. 3*C*). The P/Q type channel blocker sFTX (17) at 1 mM (Fig. 3*A*) reversibly blocked thalamic cell oscillation without affecting the low-threshold calcium spiking. Peptidyl toxin from *A. aperta* (18), at 100 nM (Fig. 3*B*), also blocked the oscillations in a reversible manner (10–20 min). These results indicate that thalamic dendritic oscillation are generated by activation of P/Q type calcium channels.

Calcium Concentration Imaging. To determine if the calcium conductances responsible for the subthreshold oscillation were preferentially located in dendrites, Fura-2 was injected intrasomatically in thalamic neurons and high-frequency oscillatory activity was evoked by direct depolarization. As illustrated in Fig. 4, high-frequency oscillations were accompanied by calcium concentration increases detected as a decrease in fluorescence at dendritic level (10). The calcium concentration image profiles coexist with the oscillatory voltage properties seen at somatic level and displayed the same voltage dependence. The localization of the calcium concentration increase, observed during neuronal oscillation, is in accordance with the decreased threshold voltage for membrane oscillation observed following barium perfusion.

DISCUSSION

The results presented here indicate that, in addition to low-threshold calcium conductance responsible for slow oscillation (1, 3), TCNs can also generate high-frequency oscillations by activating dendritic calcium conductances sensitive to P/Q channel blockers. These experiments also demonstrate that the reset of fast-membrane oscillation of TCNs can be very effectively implemented by small rapid hyperpolarizations if the cell is already oscillating (Fig. 1*E*).

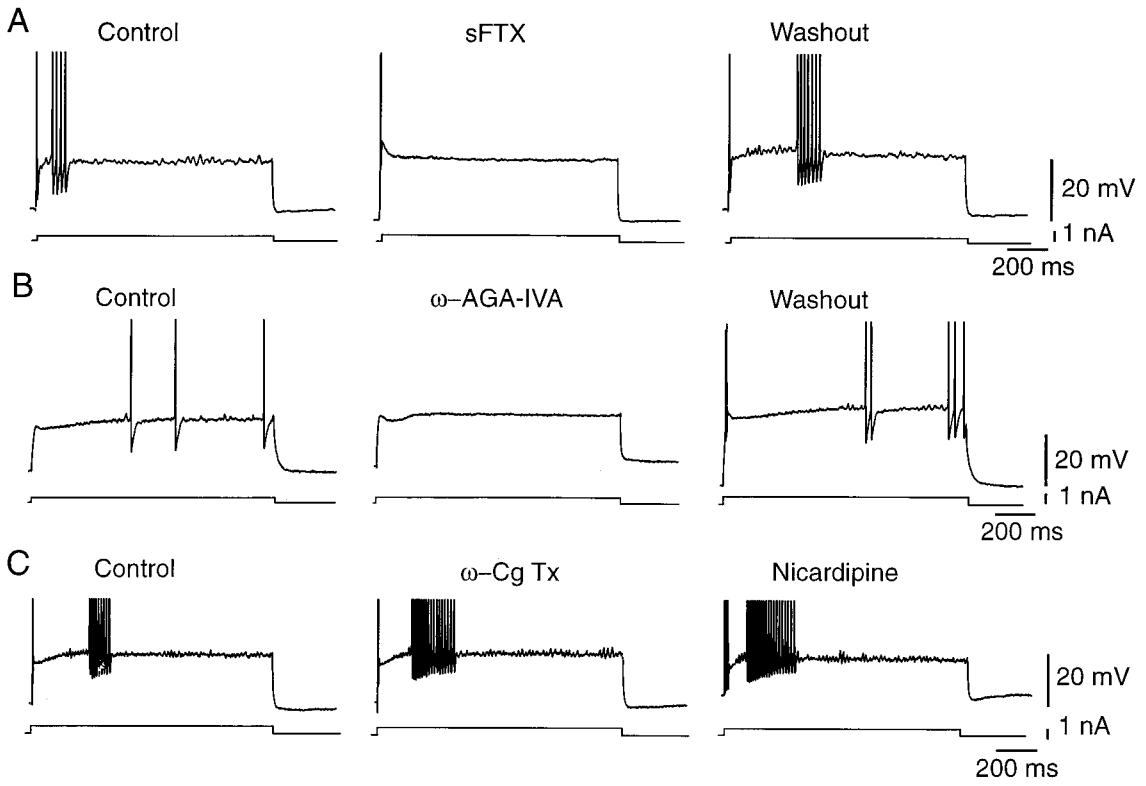

FIG. 3. Calcium channel blockers and the oscillatory activity of thalamic cells. (*A*) sFTX (1 mM) to the recording chamber completely blocked the fast subthreshold oscillations and reversed after 15 min washout. (*B*) Peptidyl toxin from *A. aperta* (100 nM) also reversibly blocked the fast oscillation. (*C*) ω-conotoxin (10 μM) or nicardipine (2 μM) had no affect on fast oscillatory activity.

From an ionic point of view, that similar gamma band oscillations can be subserved by sodium and calcium conductances in different types of neurons may imply calcium-related postsynaptic second messenger activity. Our results also suggest that gNa(p), while not involved in TCN gamma oscillations, does have a role in amplification dendritic invasion by remote depolarizations. Because most of the synaptic inputs to the TCN are dendritic, high-frequency oscillation is probably a key element in the integrative properties of these neurons. In particular, as cortical inputs are targeted predominantly in distal dendrites (19, 20), the dendritic localization of conductances underlying oscillation seem to be strategically situated to facilitate resonance with the cortical drive. In addition, it has been reported that cortical excitatory inputs to thalamic

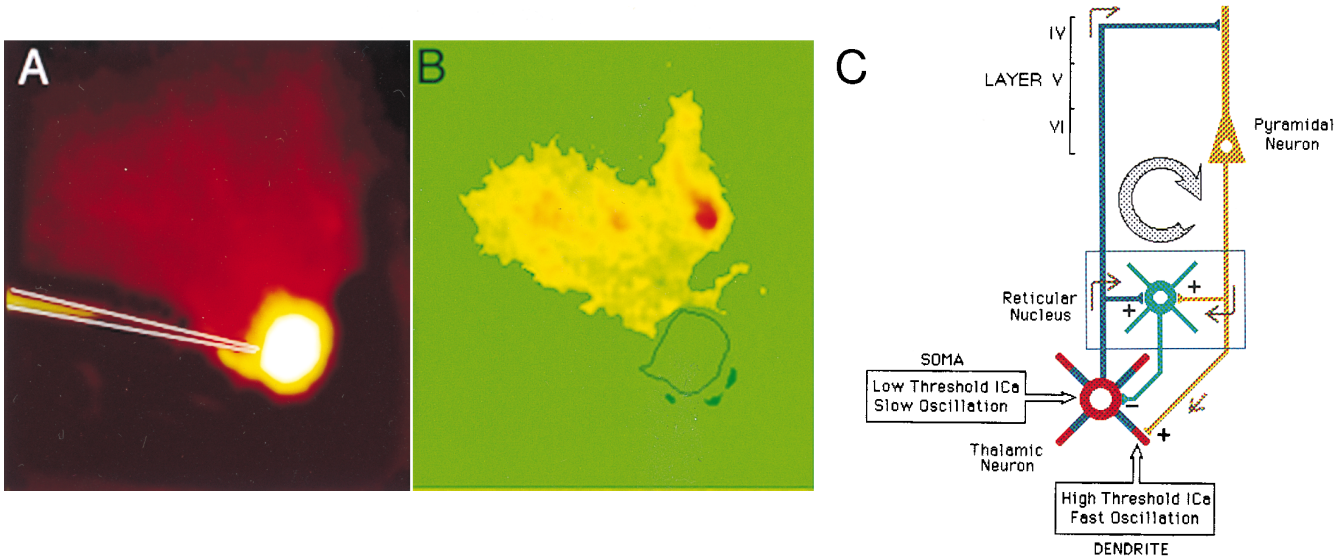

FIG. 4. Illustration of the $[Ca]_i$ location during depolarization of a thalamic cell to the level of fast membrane potential oscillations. (*A*) Fura-2 control fluorescent image of an iontophoretically filled neuron. (*B*) $[Ca]_i$ image obtained from subtracting background fluorescence from recordings acquired during a depolarizing step to membrane potential level positive to the threshold for oscillation. Note the increase in $[Ca]_i$ at dendritic level. (*C*) Diagram of the proposed thalamocortical neuronal circuit depicting the somatic and dendritic calcium conductances in thalamic neurons. A thalamic projection neuron is shown synapsing on a pyramidal cell at layer IV. The return pathway to the thalamus terminates mostly on the dendritic compartments of TCNs, where dendritic high-threshold calcium-dependent oscillations are observed (red). The corticothalamic input gives collaterals to the reticular nucleus (green) reinforcing thalamocortical resonance by inhibitory reset.

neurons are dramatically potentiated when the corticothalamic pathway is stimulated at 30–50 Hz (21). Thus, the activation of dendritic oscillation by cortical inputs may not only drive thalamic neurons but may also serve to gate inputs from other sources, allowing them to participate in the thalamocortical resonance. As such, then, thalamocortical resonance may be viewed as an emergent distributed property, which entrains the oscillatory properties at cortical and thalamic neurons, the latter mostly at dendritic level, and can bind into temporal context inputs arising from the periphery.

At another level, high-frequency oscillations close to 40 Hz have been recorded from several cortical areas (6, 22–28) and thalamic nuclei (5–7, 29–31). Moreover, coherent thalamocortical 40-Hz oscillations have been recorded from humans using magnetoencephalography (32) and from cats using local field potential, and extra- and intracellular recordings at thalamocortical level (33) but their significance is still unclear (34). Our results suggest that the TCNs may play an important role by facilitating the resonance within the thalamocortical loops and by sustaining a rhythmic drive in the network. This hypothesis is illustrated in Fig. 4*C*.

Finally, the observation that 40-Hz oscillation can be reset by short lasting outward pulses suggests that coherent short lasting inhibitory postsynaptic potentials, such as those observed spontaneously or during activated brain states (7, 11), may also reset TCNs. Moreover, synchronization and coherence of thalamocortical oscillations may be induced via reticular thalamic firing in nonbursting mode, as observed in the awake cat (35). Thus, the possibility that synaptic inputs activating recurrent inhibitory postsynaptic potentials in TCNs reset intrinsic oscillations, may go a long way in explaining the macroscopic reset of 40-Hz rhythmicity found in human magnetoencephalography studies following single sensory stimuli, as observed at both auditory and somatosensory cortex level (34).

We are particularly endebted to Prof. M. Sugimori for his help concerning the calcium imagine results and to Mr. J. Frey for technical support. This work was supported by Pew Fellowship Grant P009SC and National Institutes of Health Grant NS13742.

1. Jahnsen, H. & Llinás, R. (1984) *J. Physiol. (London)* **349,** 105–226.
2. Jahnsen, H. & Llinás, R. (1984) *J. Physiol. (London)* **349,** 227–247.
3. Leresche, N., Lightower, S., Soltesz, I., Jassik-Gerschenfeldt, D. & Crunelli, D. (1991) *J. Physiol. (London)* **441,** 155–174.
4. McCormick, D. A. & Pape, H. C. (1990) *J. Physiol. (London)* **431,** 291–318.
5. Steriade, M., Curró Dossi, R. & Contreras, D. (1993) *Neuroscience* **56,** 1–9.
6. Steriade, M., Curró Dossi, R., Paré, D. & Oakson, G. (1991) *Proc. Natl. Acad. Sci. USA* **88,** 4396–4400.
7. Pinault, D. & Deschenes, M. (1992) *Neuroscience* **51,** 245–258.
8. Llinás, R. R., Grace, A. A. & Yarom, Y. (1991) *Proc. Natl. Acad. Sci. USA* **88,** 897–901.
9. Pedroarena, C. & Llinás, R. (1996) *Soc. Neurosci. Abstr.* **22,** 356.15.
10. Sugimori, M. & Llinás, R. (1990) *Proc. Natl. Acad. Sci. USA* **87,** 5084–5088.
11. Hu, B., Steriade, M. & Deschenes, M. (1989) *Neuroscience* **31,** 13–24.
12. Alonso, A. & Llinás, R. (1989) *Nature (London)* **342,** 175–177.
13. Llinás, R. & Sugimori, M. (1980) *J. Physiol. (London)* **305,** 197–213.
14. Deisz, R. A. (1996) *Neuroscience* **70,** 341–351.
15. Hagiwara, S. & Byerly, L. (1981) *Annu. Rev. Neurosci.* **4,** 69–125.
16. Tsien, R. W., Lipscombe, D., Madison, D. V., Bley, K. R. & Fox, A. P. (1988) *Trends Neurosci.* **11,** 431–438.
17. Llinás, R., Sugimori, M., Lin, J. W. & Cherksey, B. (1989) *Proc. Natl. Acad. Sci. USA* **86,** 1689–1693.
18. Mintz, I. M., Adams, M. E. & Bean, B. P. (1992) *Neuron* **9,** 85–92.
19. Wilson, J. R., Friedlander, M. J. & Sherman, S. M. (1984) *Proc. R. Soc. London B* **221,** 411–436.
20. Liu, X. B., Honda, C. N. & Jones, E. G. (1995) *J. Comp. Neurol.* **352,** 69–91.
21. Lindström, S. & Wróbel, A. (1990) *Exp. Brain Res.* **79,** 313–318.
22. Freeman, W. J. (1978) *Electroencephalograph. Clin. Neurophysiol.* **44,** 586–605.
23. Bouyer, J. J., Montaron, M. F. & Rougeul, A. (1981) *Electroencephalograph. Clin. Neurophysiol.* **51,** 244–252.
24. Eckhorn, R., Bauer, R., Jordan, W., Brosch, M., Kruse, W., Munk, M. & Reitbock, H. J. (1988) *Biol. Cybern.* **60,** 121–130.
25. Gray, C. M. & Singer, W. (1989) *Proc. Natl. Acad. Sci. USA* **86,** 1698–1702.
26. Engel, A. K., Konig, P. & Singer, W. (1991) *Proc. Natl. Acad. Sci. USA* **88,** 9136–9140.
27. Gray, C. M., Konig, P., Engel, A. K. & Singer, W. (1989) *Nature (London)* **338,** 334–337.
28. Murthy, V. N. & Fetz, E. E. (1992) *Proc. Natl. Acad. Sci. USA* **89,** 5670–5674.
29. Adrian, E. D. & Matthews, R. (1928) *J. Physiol. (London)* **65,** 273–298.
30. Arnett, D. W. (1975) *Exp. Brain Res.* **24,** 111–130.
31. Ghose, G. M. & Freeman, R. D. (1990) *Soc. Neurosci. Abstr.* **16,** 523.4.
32. Ribary, U., Ioannides, A. A., Singh, K. D., Bolton, J. P. R., Lado, F., Mogilner, A. & Llinás, R. (1991) *Proc. Natl. Acad. Sci. USA* **88,** 11037–11041.
33. Steriade, M., Contreras, D., Amzica, F. & Timofev, I. (1996) *J. Neurosci.* **16,** 2788–2808.
34. Llinás, R. & Ribary, U. (1993) *Proc. Natl. Acad. Sci. USA* **90,** 2078–2081.
35. Steriade, M. & Deschenes, M. (1984) *Brain Res. Rev.* **8,** 1–63.